Arch Appl Mech (2021) 91:23–32
https://doi.org/10.1007/s00419-020-01795-z

TECHNICAL NOTES

Abbas Rahi

Vibration analysis of multiple-layer microbeams based on the modified couple stress theory: analytical approach

Received: 16 July 2020 / Accepted: 17 September 2020 / Published online: 28 September 2020

Abstract The modified couple stress theory (MCST) is used to capture size effect on dynamic response in multiple-layer microbeams in the present article. Governing equations of the system are obtained based on the MCST and using Hamilton's principle. The natural frequencies of the multiple-layer microbeam are calculated using the analytical method. Then, the results of the natural frequencies are presented with respect to different values of the system parameters such as the geometric layers and also the dimensionless material length-scale parameter. The results show that the material length-scale parameter values and also the length, width, and thickness of each layer are extremely effective on the vibration characteristic of the multiple-layer microbeams.

Keywords Multiple-layer microbeams · Modified couple stress theory · Size dependency · Free vibration · MEMS

1 Introduction

The vibration response study of microelectromechanical system (MEMS) devices is very important to the design and optimization of a small component of the equipment. Today, manufacturing of small size devices in the field of the MEMS is possible by the development of new knowledge and technologies. Microbeams are one of the most common elements which are used in the field of the MEMS sensors [1–9].

Several of the investigators studied the vibration response of the microcomponents in the field of MEMS based on the classical continuum mechanics theories or using the finite element method (FEM) [6,10,11]. In recent years, it has been observed that the classical continuum mechanics theories are unable to predict and explain the static and dynamic behaviors of the materials in small sizes such as microbeams [12–16]. In other words, capturing the size effect is a significant challenge in the study of the vibration response of the small size structures. Therefore, several of the non-classical continuum theories such as nonlocal elasticity theory, strain gradient theory, and couple stress theory have been offered to capture the size effect in dynamic response for microcomponents [12,17–19].

The couple stress theory was presented by Mindlin and Tiersten [18] as a non-classical continuum theory to consider the size dependency effect using two material length-scale parameters. Then, Yang et al. [19] proposed the modified couple stress theory (MCST) based on using one material length-scale parameter to capture the size effect in microcomponents.

The MCST has been used by some researchers to study the size dependency of the static and dynamic behaviors of materials in micro components. Liang et al. [20]; Park and Gao [21]; Dai et al. [22]; Ma et al. [23]; Ghiasi [24]; and Asghari et al. [25] investigated static or dynamic behaviors of micro-/nanobeams based on the MCST to capture the size dependency. Also, some researchers such as Simsek et al. [26]; He et al. [27];

A. Rahi (✉)
Faculty of Mechanical and Energy Engineering, Shahid Beheshti University, Tehran, Iran
E-mail: a_rahi@sbu.ac.ir

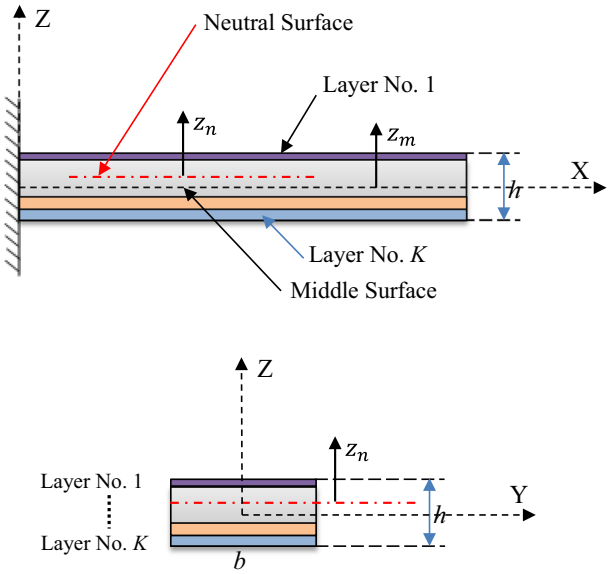

Fig. 1 Modeling of the microbeam with K layers

Guo et al. [28]; Akbas [29]; Alinaghizadeh et al. [30]; Askari and Tahani [31]; and Ghayesh and Farokhi [32] studied mechanical behaviors of microplates based on the MCST.

Shoaib et al. [33–35] investigated the dynamic response and frequency analysis and of electrostatic cantilever-based MEMS sensors without any fault. Also, Shoaib et al. [35] studied the effect of crack faults on the dynamic behavior of a piezoelectric cantilever-based MEMS sensor using the FEM approach of COMSOL tool.

In the present work, the dynamic response of a multiple-layer microbeam is investigated using an analytical approach based on the MCST. The multiple-layer microbeam is modeled by a cantilever beam with several layers that are connected together. The governing equations of the lateral vibration and the associated boundary conditions are derived based on the MCST and using Hamilton's principle. Then, the obtained governing equations are solved using an analytical approach to determine the natural frequencies of the system. Finally, the first, second, and third natural frequencies of the three-layers microbeam (one silicon layer and two piezoelectric layers) are investigated with respect to the different values of the system parameters such as the thickness of the layers, dimensionless material length-scale parameters and dimensionless parameters of the length and width of the system. The obtained results show that the material length-scale parameter values and also the length, width, and thickness of each layer have significant and interesting effects on the natural frequencies of the system.

2 Modeling and governing equations of motion

2.1 Modeling of the system

The modeling and geometry of the multiple-layer microbeam are shown in Fig. 1. The layer No. ith has length L, width b, thickness h_i, density ρ_i, Young's modulus E_i, and Poisson's ratio ϑ_i. Also, the coordinate system X–Y–Z, middle surface and neutral surface have been shown in Fig. 1.

It should be noted that for multi-layer microplates with different materials and different elasticity modulus, the middle surface (mid-plane) and the neutral surface of the cantilever beam do not coincide with each other. The z_m and z_n are the transverse coordinates defined with respect to the middle surface and neutral surface of the cantilever microplate, respectively (please see Fig. 1). The position of the neutral surface with respect to the middle surface (e) can be calculated as:

$$e = \frac{\int_{\frac{-h}{2}}^{\frac{+h}{2}} (E)(z_m)\,\mathrm{d}z_m}{\int_{\frac{-h}{2}}^{\frac{+h}{2}} E\,\mathrm{d}z_m} \tag{1}$$

For a microbeam with k layer, Eq. (1) can be written as follows:

$$e = \frac{1}{2}\frac{N_1}{\sum_{i=1}^{k}(E_i h_i)} \tag{2}$$

where

$$N_1 = \sum_{j=1}^{k} E_j \left[\left(\frac{-h}{2} + \sum_{i=j}^{k} h_i \right)^2 - \left(\frac{-h}{2} + \sum_{i=j+1}^{k} h_i \right)^2 \right] \tag{3}$$

2.2 The modified couple stress theory

The strain energy of a linear elastic isotropic material based on the modified couple stress theory can be written as follows [21,27]:

$$\pi_s = \frac{1}{2}\int_V \left(\sigma_{ij}\varepsilon_{ij} + m_{ij}\,\chi_{ij}^s \right) \mathrm{d}V\,;\ i = x,\ y,\ z\ and\ j = x,\ y,\ z \tag{4}$$

where V denotes the volume of the system. In addition, the components of the stress tensor σ_{ij}, the strain tensor ε_{ij}, the deviatoric part of the symmetric couple stress tensor m_{ij} and the symmetric curvature tensor χ_{ij}^s can be expressed as follows:

$$\sigma_{ij} = 2\mu\varepsilon_{ij} + \lambda\varepsilon_{kk}\delta_{ij}\ ;\ m_{ij} = 2\mu l^2\chi_{ij}^s \tag{5}$$

$$\varepsilon_{ij} = \frac{1}{2}\left(u_{i,j} + u_{j,i}\right)\ ;\ \chi_{ij}^s = \frac{1}{2}\left(\theta_{i,j} + \theta_{j,i}\right) \tag{6}$$

$$\theta_i = \frac{1}{2}\epsilon_{ijk}\,u_{k,j} \tag{7}$$

In the above equations, $\theta_{i,j}$ is the gradient of rotation, θ_i is infinitesimal rotation vector, ϵ_{ijk} is alternating tensor (or permutation symbol), and u_i is components of the displacement vector. The parameters (λ, μ) and l are called Lamé constants and the material length-scale parameter, respectively. The Lamé constants can also be written regarding Young's modulus E and Poisson's ratio ϑ as follows:

$$\lambda = \frac{\vartheta\,E}{(1+\vartheta)(1-2\vartheta)}\ ;\ \mu = \frac{E}{2(1+\vartheta)} \tag{8}$$

2.3 Governing equations of the system

Consider that the $w(x,t)$ denotes the transverse deflection of the neutral line of the multiple-layer microbeam with k layers at any point x along the length of the sensor in the Z direction (please see Fig. 1). By using Euler–Bernoulli beam theory, the displacement field at any material point in the microbeam can be written as follows:

$$u_1 = z_n\frac{\partial w(x,t)}{\partial x}\,;\ u_2 = 0\,;\ u_3 = w(x,t) \tag{9}$$

Assuming small transverse deflection in the multiple-layer microbeams, the nonzero components of the strain and the stress tensors can be expressed as follows:

$$\varepsilon_{xx} = z_n\frac{\partial^2 w}{\partial x^2}$$

$$\sigma_{xx} = E\varepsilon_{xx} = E_i z_n \frac{\partial^2 w}{\partial x^2}\ ;\ \text{(for layer No. } i\text{)} \tag{10}$$

The non-zero components of the symmetric curvature tensor and the deviatoric part of the symmetric couple stress tensor can be obtained as follows:

$$\begin{aligned} \chi^s_{xy} &= \chi^s_{yx} = \frac{-1}{2}\frac{\partial^2 w}{\partial x^2} \\ m_{xy} &= m_{yx} = -\frac{E_i\, l_i^2}{2\,(1+\vartheta_i)}\frac{\partial^2 w}{\partial x^2}\ ;\ \text{(for layer No. } i\text{)} \end{aligned} \tag{11}$$

where l_i is the material length-scale parameter of the layers No. i.

Therefore, from Eq. (4), the total strain energy of the system can be written as follows:

$$\begin{aligned} \pi_s &= \frac{1}{2}\int_L \left[\int_A \left(\sigma_{ij}\varepsilon_{ij} + m_{ij}\,\chi^s_{ij}\right) \mathrm{d}A\right] \mathrm{d}x \\ &= \frac{1}{2}\int_L \left[\int_A \left(\sigma_{xx}\varepsilon_{xx} + 2\,m_{xy}\,\chi^s_{xy}\right) \mathrm{d}A\right] \mathrm{d}x \\ &= \frac{1}{2}\int_0^L \left[\left(\sum_{i=1}^{K} E_i\,\tilde{I}_i\right)\left(\frac{\partial^2 w}{\partial x^2}\right)^2\right] \mathrm{d}x \\ &\quad + \frac{1}{2}\int_0^L \left[\left(\sum_{i=1}^{K} \frac{E_i\, l_i^2}{2(1+\vartheta_i)} A_i\right)\left(\frac{\partial^2 w}{\partial x^2}\right)^2\right] \mathrm{d}x \end{aligned} \tag{12}$$

where

$$\tilde{I}_i = \bar{I}_i + A_i\,\bar{z}^2_{ni}\ \bar{I}_i = \frac{b\,h_i^3}{12}\ ;\ A_i = bh_i \tag{13}$$

where

$$\begin{aligned} \bar{z}_{n1} &= \bar{z}_1 = \frac{1}{2}\,(h - 2e - h_1) \\ \bar{z}_{ni} &= \bar{z}_i = \frac{1}{2}\,(h - 2e - h_i) - \sum_{j=1}^{i-1} h_j\ ;\ \ for\ i = 2,\ ...,\ k \end{aligned} \tag{14}$$

In the above equations, A_i is the cross section area of the layers No. i at position x in length of the sensor.

It is noted that for a uniform and isotropic elastic with rectangular section $(b \times h_i)$, the cross-sectional area–moment of inertia about yy axis can be calculated from $\bar{I}_i = \frac{bh_i^3}{12} = \frac{A_i\,h_i^2}{12}$ for $i = 1,\ 2,\ ...,\ K$. Therefore, according to Eq. (10), the total strain energy of the system can be written as follows:

$$\pi_s = \frac{1}{2}\left\{\left(\sum_{i=1}^{K} E_i\,\tilde{I}_i\right) + \left[\sum_{i=1}^{K} \frac{6\,E_i\,\bar{I}_i}{(1+\vartheta_i)}\left(\frac{l_i}{h_i}\right)^2\right]\right\}\int_0^L \left[\left(\frac{\partial^2 w}{\partial x^2}\right)^2\right] \mathrm{d}x \tag{15}$$

The kinetic energy of the system T can be written as follows:

$$T = \frac{1}{2}\int_0^L \left[\left(\sum_{i=1}^{K} \rho_i A_i\right)\dot{w}^2 + \left(\sum_{i=1}^{K} \rho_i\,\tilde{I}_i\right)\left(\frac{\partial \dot{w}}{\partial x}\right)^2\right] \mathrm{d}x \tag{16}$$

where the dot over variables is the derivative of variable relative to time.

Hamilton's principle is considered as follows:

$$\int_{t1}^{t2} \delta\,(T - \pi_s + W)\ \mathrm{d}t = 0 \tag{17}$$

where δW is the virtual work done by external non-conservative forces on the system. For free vibration analysis of the considered system, the δW is zero.

By substituting Eqs. (15) and (16) into (17), and then using variational calculus, governing equations of motion of the system can be derived as follows:

$$S\frac{\partial^4 w}{\partial x^4} + B\,\ddot{w} - D\frac{\partial^2 \ddot{w}}{\partial x^2} = 0 \tag{18}$$

where

$$\begin{aligned} S &= \sum_{i=1}^{K} E_i\,\tilde{I}_i + \sum_{i=1}^{K} \frac{6\,E_i\,\bar{I}_i}{(1+\vartheta_i)}\left(\frac{l_i}{h_i}\right)^2 \\ B &= \sum_{i=1}^{K} \rho_i A_i = \sum_{i=1}^{K} \rho_i\, b\, h_i \\ D &= \sum_{i=1}^{K} \rho_i\,\tilde{I}_i \end{aligned} \tag{19}$$

By neglecting $\frac{\partial^2 \ddot{w}}{\partial x^2}$, the Eq. (18) can be simplified as follows:

$$S\frac{\partial^4 w}{\partial x^4} + B\,\ddot{w} = 0 \tag{20}$$

The solution of Eq. (17) can be expressed as follows:

$$w\,(x,t) = W\,(x) \times sin\,(\omega t) \tag{21}$$

By substituting Eq. (21) into Eq. (20) and to have some algebraic simplification, we have

$$\begin{aligned} &\frac{\mathrm{d}^4 W}{\mathrm{d}x^4} - \beta^4 W\,(x) = 0 \\ &\beta^4 = \frac{B\,\omega^2}{S} \end{aligned} \tag{22}$$

where ω is the natural frequency. Also, the general solution of Eq. (22) can be obtained as follows:

$$W\,(x) = \tilde{B}_1 \sin\,(\beta x) + \tilde{B}_2 \cos\,(\beta x) + \tilde{B}_3 \sinh\,(\beta x) + \tilde{B}_4 \cosh\,(\beta x) \tag{23}$$

where $\tilde{B}_1$, $\tilde{B}_2$, $\tilde{B}_3$, and $\tilde{B}_4$ are constants.

Also, the boundary conditions of the system can be expressed as follows:

$$\begin{aligned} W\,(0) = 0\ ;\ \frac{\mathrm{d}W}{\mathrm{d}x}\,(0) = 0 \\ \frac{\mathrm{d}^2 W}{\mathrm{d}x^2}\,(L) = 0\ ;\ \frac{\mathrm{d}^3 W}{\mathrm{d}x^3}\,(L) = 0 \end{aligned} \tag{24}$$

By substituting Eq. (24) into Eq. (23), a set of four algebraic equations resulting in matrix form can be obtained as follows:

$$\left[Q_{ij}\right]\left\{\tilde{B}_j\right\} = 0\ ;\ \ i,\ j = 1,\ 2,\ 3,\ 4 \tag{25}$$

where

$$\begin{aligned} &Q_{11} = Q_{13} = 0\,;\ Q_{12} = Q_{14} = 1 \\ &Q_{22} = Q_{24} = 0\,;\ Q_{21} = Q_{23} = -\beta \\ &Q_{31} = -\beta^2 \sin\,(\beta L)\ ;\ Q_{32} = -\beta^2 \cos\,(\beta L) \end{aligned}$$

$$
\begin{aligned}
&Q_{33} = \beta^2 \sinh(\beta L) \; ; \; Q_{34} = \beta^2 \cosh(\beta L) \\
&Q_{41} = -\beta^3 \cos(\beta L) \; ; \; Q_{42} = \beta^3 \sin(\beta L) \\
&Q_{43} = \beta^3 \cosh(\beta L) \; ; \; Q_{44} = \beta^3 \sinh(\beta L)
\end{aligned} \tag{26}
$$

For nontrivial solution of Eq. (25), the determinant of the matrix $\left[Q_{ij}\right]$ must be zero. Also, if the determinant of the matrix $\left[Q_{ij}\right]$ be zero, the result and the first, second, third, and fourth roots of it can be calculated as follows:

$$
\begin{aligned}
&det\left[Q_{ij}\right] = 0 \Rightarrow \cos(\beta_n L)\cosh(\beta_n L) = -1 \; ; \; n = 1, \ldots, \infty \\
&\beta_1 L = 1.87510 \; ; \; \beta_2 L = 4.69409 \; ; \; \beta_3 L = 7.85476 \; ; \; \beta_4 L = 10.99554
\end{aligned} \tag{27}
$$

Therefore, according to Eqs. (22) and (27), the natural frequencies of the multiple-layer microbeams with k layers can be determined as follows:

$$
\omega_n = (\beta_n L)^2 \left[\frac{S}{B\,L^4}\right]^{\frac{1}{2}} = (\beta_n L)^2 \left[\frac{S}{\left(\sum_{i=1}^{K} \rho_i h_i\right) L^4}\right]^{\frac{1}{2}} \tag{28}
$$

where

$$
S = \sum_{i=1}^{K} E_i h_i \left(\frac{h_i^2}{12} + \bar{z}_i^2\right) + \sum_{i=1}^{K} \frac{E_i h_i^3}{2(1+\vartheta_i)} \left(\frac{l_i}{h_i}\right)^2 \tag{29}
$$

3 Verification

In the previous section, the governing equation of motion for lateral vibration of the cantilever multiple-layer microbeams with k layers which are connected together was derived analytically based on the MCST as follows:

$$
\left[\sum_{i=1}^{K} E_i \tilde{I}_i + \sum_{i=1}^{K} \frac{6\,E_i \bar{I}_i}{(1+\vartheta_i)} \left(\frac{l_i}{h_i}\right)^2\right] \frac{\partial^4 w}{\partial x^4} + \left(\sum_{i=1}^{K} \rho_i A_i\right) \ddot{w} = 0 \tag{30}
$$

where

$$
\begin{aligned}
\tilde{I}_i &= \bar{I}_i + A_i\,\bar{z}_{ni}^2 \; ; \; \text{for}\, i = 1, 2, \ldots, K \\
\bar{I}_i &= \frac{b\,h_i^3}{12} \; ; \; A_i = b h_i \; ; \; \text{for}\, i = 1, 2, \ldots, K \\
\bar{z}_{n1} &= \frac{1}{2}(h - 2e - h_1) \\
\bar{z}_{ni} &= \frac{1}{2}(h - 2e - h_i) - \sum_{j=1}^{i-1} h_j \; ; \; \text{for}\, i = 2, \ldots, k
\end{aligned} \tag{31}
$$

In special case $\frac{l_i}{h_i} \approx 0$, for the macrosystem, Eq. (30) is simplified as

$$
\left(\sum_{i=1}^{K} E_i \tilde{I}_i\right) \frac{\partial^4 w}{\partial x^4} + \left(\sum_{i=1}^{K} \rho_i A_i\right) \ddot{w} = 0 \tag{32}
$$

Also, It can be easily seen that for the special case $h_i = 0\,(for\, i \neq 1)$ (when we have only one layer), Eq. (32) is simplified as

$$
\left(E_1 \bar{I}_1\right) \frac{\partial^4 w}{\partial x^4} + (\rho_1 A_1)\, \ddot{w} = 0 \tag{33}
$$

Equation (33) is compatible with the classical form of the governing equations of free vibration of a cantilever beam in macro size.

Table 1 Dimensions and material parameters of the microbeam with 3 layers

Parameters description	Symbol	unit	Layer No. 1 (Piezoelectric layer) $i = 1$	Layer No. 2 (Silicon layer) $i = 2$	Layer No. 3 (Piezoelectric layer) $i = 3$
Length	L	μm	800	800	800
Width	b	μm	300	300	300
Thickness	h_i	μm	10	20	10
Young's modulus	E_i	GPa	63	170	63
Density	ρ_i	Kg/m^3	7550	2233	7550
Poisson's ratio	ϑ_i	–	0.32	0.22	0.32

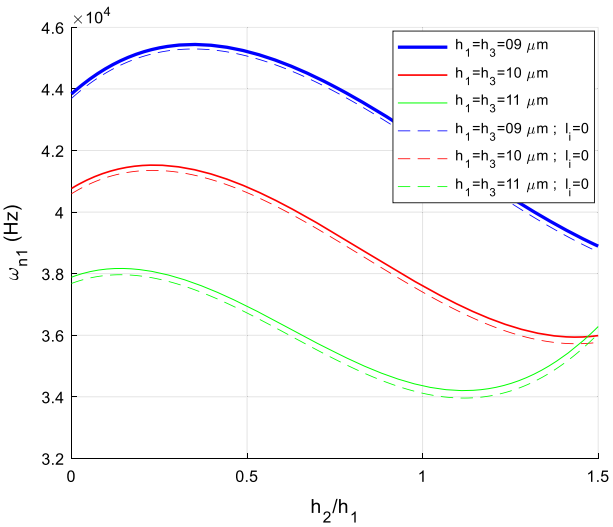

Fig. 2 Variation of the first natural frequency of the multiple-layer microbeam versus the ratio thickness of layers $\frac{h_2}{h_1}$ for different values of the layer thickness h_1 and h_3

4 Results and discussion

In this section, the effect of size and also dimensions of the multiple-layer microbeam with three layers (two layers of piezoelectric and one layer of silicon) on the natural frequencies of the system are studied. In numerical analyses, according to Fig. 1, the nominal dimensions, materials, and geometry of the multiple-layer microbeam are mentioned in Table 1 [35].

In the present paper, the material length-scale parameter l_i for silicon and piezoelectric layers has been considered 1.0μm and 2.4μm, respectively [35].

The first natural frequency of the multiple-layer microbeam versus the ratio thickness of the silicon layer to thickness of the piezoelectric layer $\left(\frac{h_2}{h_1}\right)$ has been presented in Fig. 2, for different values of the layer thickness h_1 and h_3. The obtained results in Fig. 2 show that there is interesting behavior on the natural frequencies with the increase in dimensionless thickness parameter h_2/h_1 . It should be noted that this behavior can be considered in the optimization design of the multiple-layer microbeam such as microsensors system. The above behavior for second and third natural frequencies of the multiple-layer microbeam can also be observed in Figs. 3 and 4, respectively.

Also, the first natural frequency of the multiple-layer microbeam versus piezoelectric thickness h_3 has been depicted in Fig. 5 for various values of dimensionless material length-scale parameter l_2/h_2, at silicon thickness $h_1 = 10\,\mu$m and $h_2 = 20\,\mu$m.

In addition, the variation of the first natural frequency of the system versus the parameter h_2 has been studied in Fig. 6 for different values of the thickness $of\ the\ layers\ h_1$ and h_3 , at microbeam length $L = 800\,\mu$m. The obtained results in Fig. 6 show that the first natural frequency of the multiple-layer microbeam will increase when dimensionless parameter h_2 increases.

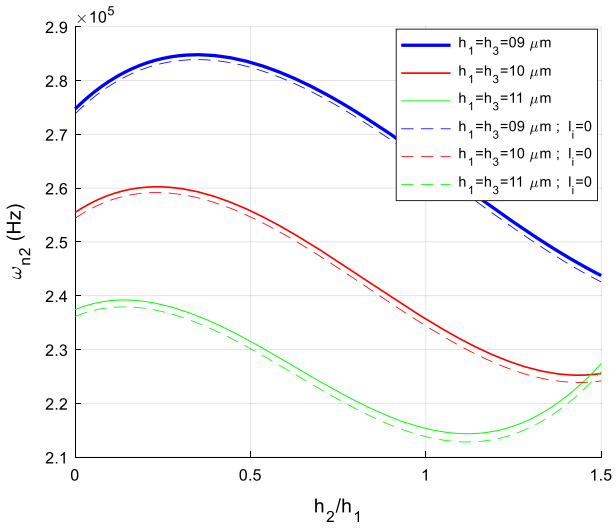

Fig. 3 Variation of the second natural frequency of the multiple-layer microbeam versus the ratio thickness of layers $\frac{h_2}{h_1}$ for different values of the layer thickness h_1 and h_3

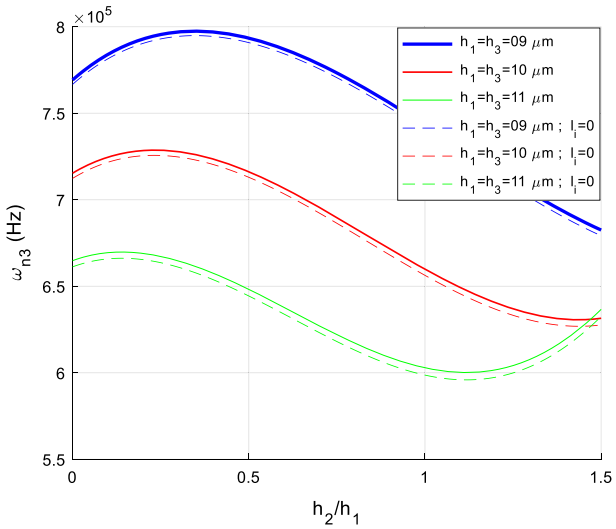

Fig. 4 Variation of the third natural frequency of the multiple-layer microbeam versus the ratio thickness of layers $\frac{h_2}{h_1}$ for different values of the layer thickness h_1 and h_3

In Figures 2, 3, 4, 5 and 6, the results of the higher-order theory have been presented with solid lines, and dashed lines have been used for the curves with the vanishing the material length-scale parameters l_i.

5 Summary and conclusion

In this article, the dynamic response of a multiple-layer microbeam was studied by an analytical approach. To capture size effects and also to predict the vibration response of the multiple-layer microbeam, governing equations were derived based on Hamilton's principle and modified couple stress theory (MCST). The analytical approach was used in the solution of the partial differential equations. The first, second, and third natural frequencies of the system for various values of system parameters such as dimensionless material length-scale parameter, the thickness of the silicon, and piezoelectric layers, were investigated.

The obtained results of the natural frequencies were presented for a multiple-layer microbeam with one silicon layer and two piezoelectric layers. The results show that material length-scale parameter values and

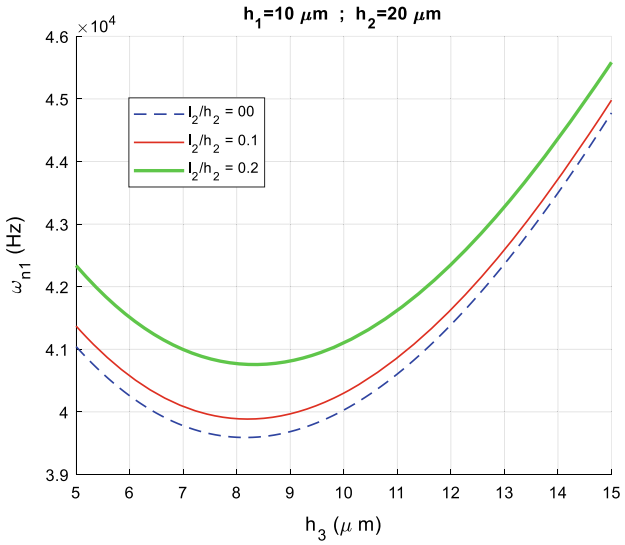

Fig. 5 Variation of the first natural frequency of the multiple-layer microbeam versus thickness of the piezoelectric layer h_3 for different values of dimensionless material length-scale parameter l_2/h_2

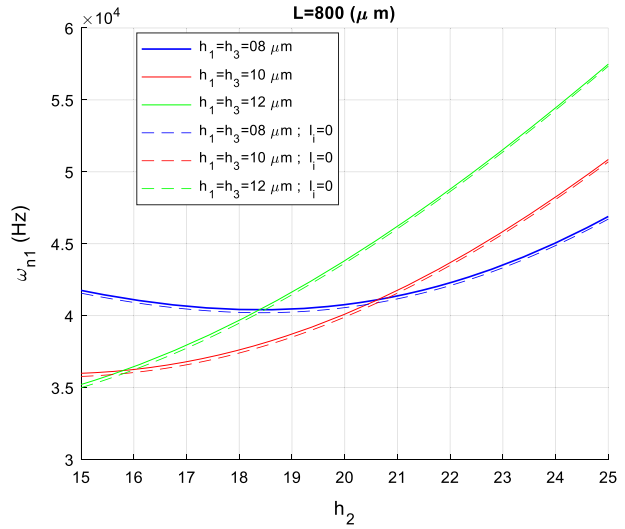

Fig. 6 Variation of the first natural frequency of the multiple-layer microbeam versus the parameter h_2 for different values of the thickness $of\ the\ layers\ h_1$ and h_3

also the length, width, and thickness of each layer have significant effects on the vibration behavior of the multiple-layer microbeam system.

References

1. Rezazadeh, G., Tahmasebi, A., Zubstov, M.: Application of piezoelectric layers in electrostatic MEM actuators: controlling of pull-in voltage. Microsyst. Technol. **12**(12), 1163–1170 (2006)
2. Hu, Y.C., Chang, C.M., Huang, S.C.: Some design considerations on the electrostatically actuated microstructures. Sens. Actuat. A **112**(1), 155–161 (2004)
3. Mahdavi, M.H., Farshidianfar, A., Tahani, M., Mahdavi, S., Dalir, H.: A more comprehensive modeling of atomic force microscope cantilever. Ultramicroscopy **109**(1), 54–60 (2008)
4. Lun, F.Y., Zhang, P., Gao, F.B., Jia, H.G.: Design and fabrication of micro-optomechanical vibration sensor. Microfabr. Technol. **120**(1), 61–64 (2006)

5. McMahan, L.E., Castleman, B.W.: Characterization of vibrating beam sensors during shock and vibration. In: Position Location and Navigation Symposium. PLANS 2004. IEEE, pp. 102–110 (2004)
6. Coutu, R.A., Kladitis, P.E., Starman, L.A., Reid, J.R.: A comparison of micro-switch analytic, finite element, and experimental results. Sens. Actuat. A **115**(2), 252–258 (2004)
7. Duc, T.C., Creemer, J.F., Sarro, P.M.: Piezoresistive cantilever beam for force sensing in two dimensions. Sens. J. IEEE **7**, 96–104 (2007)
8. Abdel-Rahman, E.M., Younis, M.I., Nayfeh, A.H.: Characterization of the mechanical behavior of an electrically actuated microbeam. J. Micromech. Microeng. **12**(6), 759–766 (2002)
9. Zand, M.M., Ahmadian, M.T.: Vibrational analysis of electrostatically actuated microstructures considering nonlinear effects. Commun. Nonlinear Sci. Numer. Simul. **14**(4), 1664–1678 (2009)
10. Orhan, S.: Analysis of free and forced vibration of a cracked cantilever beam. NDT & E Int. **40**, 443–450 (2007)
11. Barad, K.H., Sharma, D.S., Vyas, V.: Crack detection in cantilever beam by frequency based method. Proc. Eng. **51**, 770–775 (2013)
12. Lam, D.C., Yang, F., Chong, A.C.M., Wang, J., Tong, P.: Experiments and theory in strain gradient elasticity. J. Mech. Phys. Solids **51**(8), 1477–1508 (2003)
13. Fleck, N.A., Muller, G.M., Ashby, M.F., Hutchinson, J.W.: Strain gradient plasticity: theory and experiment. Acta Metall. Mater. **42**(2), 475–487 (1994)
14. Stölken, J.S., Evans, A.G.: A microbend test method for measuring the plasticity length scale. Acta Mater. **46**(14), 5109–5115 (1998)
15. Lam, D.C., Chong, A.C.: Indentation model and strain gradient plasticity law for glassy polymers. J. Mater. Res. **14**(09), 3784–3788 (1999)
16. Chong, A.C., Lam, D.C.: Strain gradient plasticity effect in indentation hardness of polymers. J. Mater. Res. **14**(10), 4103–4110 (1999)
17. Eringen, A.C.: Nonlocal polar elastic continua. Int. J. Eng. Sci. **10**(1), 1–16 (1972)
18. Mindlin, R.D., Tiersten, H.F.: Effects of couple-stresses in linear elasticity. Arch. Ration. Mech. Anal. **11**(1), 415–448 (1962)
19. Yang, F.A.C.M., Chong, A.C.M., Lam, D.C., Tong, P.: Couple stress based strain gradient theory for elasticity. Int. J. Solids Struct. **39**(10), 2731–2743 (2002)
20. Liang, L.N., Ke, L.L., Wang, Y.S., Yang, J., Kitipornchai, S.: Flexural vibration of an atomic force microscope cantilever based on modified couple stress theory. Int. J. Struct. Stab. Dyn. **15**(07), 1540025 (2015)
21. Park, S.K., Gao, X.L.: Bernoulli–Euler beam model based on a modified couple stress theory. J. Micromech. Microeng. **16**(11), 2355–2359 (2006)
22. Dai, H.L., Wang, Y.K., Wang, L.: Nonlinear dynamics of cantilevered microbeams based on modified couple stress theory. Int. J. Eng. Sci. **94**, 103–112 (2015)
23. Ma, H.M., Gao, X.L., Reddy, J.N.: A microstructure-dependent Timoshenko beam model based on a modified couple stress theory. J. Mech. Phys. Solids **56**(12), 3379–3391 (2008)
24. Ghiasi, E.K.: Application of modified couple stress theory to study dynamic characteristics of electrostatically actuated micro-beams resting upon squeeze-film damping under mechanical shock. Int. J. Adv. Mech. Eng. **6**(1), 1–15 (2016)
25. Asghari, M., Kahrobaiyan, M.H., Rahaeifard, M., Ahmadian, M.T.: Investigation of the size effects in Timoshenko beams based on the couple stress theory. Arch. Appl. Mech. **81**(7), 863–874 (2011)
26. Simsek, M., Aydın, M.: Size-dependent forced vibration of an imperfect functionally graded (FG) microplate with porosities subjected to a moving load using the modified couple stress theory. Compos. Struct. **160**, 408–421 (2017)
27. He, D., Yang, W., Chen, W.: A size-dependent composite laminated skew plate model based on a new modified couple stress theory. Acta Mech. Solida Sin. **30**(1), 75–86 (2017)
28. Guo, J., Chen, J., Pan, E.: Free vibration of three-dimensional anisotropic layered composite nanoplates based on modified couple-stress theory. Physica E **87**, 98–106 (2017). https://doi.org/10.1016/j.physe.2016.11.025
29. Akbas, S.D.: Free vibration of edge cracked functionally graded microscale beams based on the modified couple stress theory. Int. J. Struct. Stab. Dyn. **17**(03), 1750033 (2017)
30. Alinaghizadeh, F., Shariati, M., Fish, J.: Bending analysis of size-dependent functionally graded annular sector microplates based on the modified couple stress theory. Appl. Math. Model. (2017). https://doi.org/10.1016/j.apm.2017.02.018
31. Askari, A.R., Tahani, M.: Size-dependent dynamic pull-in analysis of geometric non-linear micro-plates based on the modified couple stress theory. Physica E **86**, 262–274 (2017). https://doi.org/10.1016/j.physe.2016.10.035
32. Ghayesh, M.H., Farokhi, H.: Nonlinear dynamics of microplates. Int. J. Eng. Sci. **86**, 60–73 (2015)
33. Shoaib, M., Hisham, N., Basheer, N., Tariq, M.: Frequency analysis of electrostatic cantilever-based MEMS sensor. In: Symposium on Design, Test, Integration and Packaging of MEMS/MOEMS (DTIP), pp. 1–6 (2015)
34. Shoaib, M., Hisham, N., Basheer, N., Tariq, M.: Frequency and displacement analysis of electrostatic cantilever-based MEMS sensor. In: Analog Integrated Circuits and Signal Processing, pp. 1–11 (2016)
35. Shoaib, M., Hamid, N.H., Jan, M.T., Ali, N.B.Z.: Effects of crack faults on the dynamics of piezoelectric cantilever-based MEMS sensor. IEEE Sens. J. **17**(19), 6279–6294 (2017)